IOPscience iopscience.iop.org

Home Search Collections Journals About Contact us My IOPscience

Electron-interface phonon scattering in $GaAs/Ga_{1-x}Al_xAs$ quantum-well structures with interface roughness

This article has been downloaded from IOPscience. Please scroll down to see the full text article.

1993 J. Phys.: Condens. Matter 5 2859

(http://iopscience.iop.org/0953-8984/5/18/007)

View the table of contents for this issue, or go to the journal homepage for more

Download details:
IP Address: 171.66.16.159
The article was downloaded on 12/05/2010 at 13:17

Please note that terms and conditions apply.

J. Phys.: Condens. Matter 5 (1993) 2859–2868. Printed in the UK

Electron–interface phonon scattering in $GaAs/Ga_{1-x}Al_xAs$ quantum-well structures with interface roughness

Wenhui Duan†, Jia-Lin Zhu‡ and Bing-Lin Gu‡

† Department of Physics, Tsinghua University, Beijing 100084, People's Republic of China
‡ Centre of Theoretical Physics, Chinese Centre of Advanced Science and Technology (World Laboratory), PO Box 8730, Beijing 100080, and § Department of Physics, Tsinghua University, Beijing 100084, People's Republic of China

Received 17 November 1992

Abstract. Considering the influence of interface roughness on phonon vibrational modes in the dielectric continuum model, electron–interface phonon scattering rates are calculated in a model $GaAs/Ga_{1-x}Al_xAs$ quantum-well structure. The intrasubband and intersubband scattering rates are given as a function of quantum-well width. It is shown that interface phonon scattering is the dominant scattering mechanism in narrow quantum-well structures and electron relaxation is strongly dependent on interface roughness. For intersubband scattering, the infinite barrier height approximation can introduce a large error, in particular, in narrow quantum-well structures. Our results are in good agreement with recent experimental data.

1. Introduction

The novel features of semiconductor superlattices and multiple quantum wells have led to a great deal of interest in their electronic and optical vibrational properties. The presence of a hetero-interface gives rise to confinement of optical phonons in each layer and localization in the vicinity of interfaces. The first unambiguous observation of phonons confined in GaAs slabs was made in 1984 (Jusseraud *et al* 1984), and interface phonons in GaAs–AlAs superlattices were discovered in 1985 (Sood *et al* 1985). Both macroscopic and microscopic approaches to confined phonons have been applied in theoretical treatments (Huang and Zhu 1988a,b), and the frequency and dispersion of the interface modes can be analysed in terms of a dielectric continuum model (Fuchs and Kliewer 1965, Wendler 1985, Chen *et al* 1990). It has been shown that in some respects the continuum model gives a reasonably good representation of these modes. It should be pointed out that the atomic-scale morphology of interfaces and the interface effect on quantum-well structures have not been completely considered to date as the continuum model has been used. In a vapour-deposited multilayer, in fact, interface roughness may arise from a variety of factors, including substrate roughness, rate fluctuations, island growth mode, interdiffusion, etc. The atomic-scale morphology of a semiconductor interface is still controversial, even for the $GaAs/Ga_{1-x}Al_xAs$ system, which has been intensively studied for many years. However, interface roughness can be divided into component roughness and structure roughness. The component roughness means the chemical component difference between ideal and real interfaces and may be induced by chemical composition fluctuation of monolayers,

§ Address for correspondence.

0953-8984/93/182859+10$07.50 © 1993 IOP Publishing Ltd

interdiffusion, etc. For a sample with good quality, we think that it is more important for subbands and related excitons (Zhu *et al* 1989) and interface modes and related electron–optical phonon interactions than is structure roughness. Therefore, it is interesting to study the influence of component roughness on these.

Recently there has been considerable attention given to the subject of electron–phonon scattering and electron relaxation in GaAs/$Ga_{1-x}Al_xAs$ multiple-quantum-well structures (Tatham *et al* 1989, Obreli *et al* 1987, Seilmeier *et al* 1987, Ridley 1989, Rudin and Reinecke 1990, Dharssi and Butcher 1990). The corresponding electron scattering rates have been studied experimentally by time-resolved Raman scattering (Tatham *et al* 1989, Obreli *et al* 1987) and infrared spectroscopy (Seilmeier *et al* 1987). There have been suggestions that interactions by the interface modes can be significant and that the scattering rate due to the confined modes can be considerably reduced in some structures compared to the bulk LO phonon scattering rate (Stroscio *et al* 1991). However, almost no attention has been paid to the effect of the component roughness, mentioned above, on interface modes and related electron–optical phonon interaction. It would be expected to be particularly important for electron relaxation and mobility because a component change at the interface can cause a large change of interface modes and make the envelope wavefunction of the highest subband more extended. Therefore, it should be worthwhile to study the effect of such roughness both experimentally and theoretically. This can also allow us to analyse quantitatively the atomic-scale component of the interfaces.

In the present paper, we consider the effect of interface component roughness on electron envelope subband wavefunctions and phonon vibrational modes, and calculate intrasubband and intersubband electron–interface phonon scattering in a model GaAs/$Ga_{1-x}Al_xAs$ quantum-well structure. The electron envelope subband wavefunctions are obtained in structures with both finite and infinite barrier height, and the finite barrier height effect on scattering is also studied. In order to check the interface model structure, calculated results are compared with experimental data. The results can be used to discuss the validity of different macroscopic and microscopic approaches to the confined phonon in conjunction with experiments.

2. Interface phonon modes and electron subbands

Let us for definiteness consider a GaAs or $Ga_{1-x}Al_xAs$ layer i ($i = 1, 2, 3, \ldots$) of the GaAs/$Ga_{1-x}Al_xAs$ system. It has the optical dielectric constant $\epsilon_{\infty i}$, the LO frequency ω_{Li} and the TO frequency ω_{Ti}. The z axis is taken to be perpendicular to the interfaces. Within the framework of the continuum model, the equation of motion and polarization eigenmodes can be obtained (Wendler 1985, Chen *et al* 1990). Introducing the electric field component $E_k(\boldsymbol{k}, z)$ and the electric displacement component $D_z(\boldsymbol{k}, z)$, where $\boldsymbol{k}$ is the in-plane component of the phonon wavevector, we have

$$D_{zi}(\boldsymbol{k}, z) = \epsilon_i(\omega)\frac{\mathrm{d}}{\mathrm{d}z}E_{ki}(\boldsymbol{k}, z)/\mathrm{i}k \tag{1a}$$

and

$$\begin{aligned}\frac{\mathrm{d}^2}{\mathrm{d}z^2}D_{zi}(\boldsymbol{k}, z) &= k^2 D_{zi}(\boldsymbol{k}, z)\\ \frac{\mathrm{d}^2}{\mathrm{d}z^2}E_{ki}(\boldsymbol{k}, z) &= k^2 E_{ki}(\boldsymbol{k}, z)\end{aligned} \qquad (i = 1, 2, \ldots, N) \tag{1b}$$

with

$$\epsilon(\omega) = \epsilon_i(\omega) = \epsilon_{\infty i}(\omega_{\mathrm{L}i}^2 - \omega^2)/(\omega_{\mathrm{T}i}^2 - \omega^2). \tag{2}$$

For the ith layer, it is easier to solve the equations and obtain

$$\begin{aligned} E_{ki}(\boldsymbol{k}, z) &= \mathrm{i}(A_i \mathrm{e}^{kz} - B_i \mathrm{e}^{-kz}) \\ D_{zi}(\boldsymbol{k}, z) &= \epsilon_i(\omega)(A_i \mathrm{e}^{kz} + B_i \mathrm{e}^{-kz}). \end{aligned} \tag{3}$$

However, for the first and last material layers in the GaAs/Ga$_{1-x}$Al$_x$As quantum-well structures, the solutions are respectively

$$\begin{aligned} E_{k0}(\boldsymbol{k}, z) &= \mathrm{i}A_0 \mathrm{e}^{kz} \\ D_{z0}(\boldsymbol{k}, z) &= \epsilon_0(\omega) A_0 \mathrm{e}^{kz} \end{aligned} \tag{4}$$

and

$$\begin{aligned} E_{k,N+1}(\boldsymbol{k}, z) &= -\mathrm{i}B_{N+1} \mathrm{e}^{-kz} \\ D_{z,N+1}(\boldsymbol{k}, z) &= \epsilon_{N+1}(\omega) B_{N+1} \mathrm{e}^{-kz}. \end{aligned} \tag{5}$$

This is reasonable for studies of the interface roughness effect on the optical phonon. By using the connection conditions of $E_k(\boldsymbol{k}, z)$ and $D_z(\boldsymbol{k}, z)$ with the help of the 2×2 transfer matrices, it is convenient to obtain the equation of the eigenvalues. It is as follows:

$$T_{21} + T_{22}\epsilon_0(\omega) + \epsilon_{N+1}(\omega)[T_{11} + T_{12}\epsilon_0(\omega)] = 0 \tag{6}$$

where T_{ij} is an element of the 2×2 matrix, i.e.

$$T = \begin{bmatrix} T_{11} & T_{12} \\ T_{21} & T_{22} \end{bmatrix} = Q_N S_{N-1} Q_{N-1} \ldots S_1 Q_1 S_0 \tag{7}$$

with

$$S_i = \begin{bmatrix} 1 & \epsilon_{i+1}^{-1}(\omega) \\ -1 & \epsilon_{i+1}^{-1}(\omega) \end{bmatrix} \tag{8a}$$

and

$$Q_i = \begin{bmatrix} \exp(kd_i) & -\exp(-kd_i) \\ \epsilon_i(\omega)\exp(kd_i) & \epsilon_i(\omega)\exp(-kd_i) \end{bmatrix}. \tag{8b}$$

Here d_i and N are, respectively, the ith layer width and the layer number of the well region. Once the eigenvalue ω_ν is known, the A_0, A_i, B_i ($i = 1, 2, \ldots, N$) and B_{N+1} (hence $E_k(\boldsymbol{k}, z)$ and $D_z(\boldsymbol{k}, z)$) are known with the use of the 2×2 transfer matrices and the normalization condition (Wendler 1985).

Effective-mass theory is used to calculate the subband wavefunctions of electron states. The envelope subband wavefunction in the ith layer satisfies:

$$\frac{\hbar^2}{2m_i}\frac{\mathrm{d}\Psi_i^2}{\mathrm{d}z^2} + V_i\Psi_i = E_e\Psi_i \tag{9}$$

where V_i and m_i are respectively the potential barrier height and the effective mass of an electron in the ith layer. Then, the solutions are as follows:

$$\Psi_i = C_i f_i(z) + D_i g_i(z) = \begin{cases} C_i \sin(k_{ei} z) + D_i \cos(k_{ei} z) & \text{for } V_i < E_e \\ C_i \exp(k_{ei} z) + D_i \exp(-k_{ei} z) & \text{for } V_i > E_e \end{cases} \tag{10}$$

with

$$k_{ei} = [(2m_i/\hbar^2)|E - V_i|]^{1/2}. \tag{11}$$

However, for the first and the last material layers (potential barrier layers) in a $GaAs/Ga_{1-x}Al_xAs$ quantum-well structure, the solutions are respectively

$$\begin{aligned} \Psi_0 &= C_0 \exp(k_{ei} z) \\ \Psi_{N+1} &= D_{N+1} \exp(-k_{ei} z). \end{aligned} \tag{12}$$

Considering the continuity of Ψ and $(1/m)\,\mathrm{d}\Psi/\mathrm{d}z$ with the help of 2×2 transfer matrices, the equation of the eigenvalues for the electron can be obtained in a calculation procedure similar to that of the interface modes calculation. It is interesting to point out that the similarity of the calculation method for the electron wavefunction and interface modes will make it convenient to calculate the scattering rate.

3. The electron–interface phonon scattering

The electron–phonon interaction Hamiltonian derived from Fröhlich interaction is given by (Huang and Zhu 1988b, Wendler 1985, Licari and Evrard 1977)

$$H_{ep} = \sum_{\nu} \sum_{k} \left(\frac{\hbar e^2}{2A\omega_\nu(k)} \right)^{1/2} \frac{\mathrm{i}}{k} E_k^\nu(k, z) \mathrm{e}^{\mathrm{i}k\cdot\rho} [a_\nu(k) + a_\nu^+(-k)] \tag{13}$$

where a_ν and a_ν^+ are, respectively, the annihilation and creation operators of an optical phonon, and A is unit area of the quantum-well system in the xy plane. Considering a one-phonon process only in the standard manner, the scattering rate is obtained as follows:

$$\begin{aligned} W(k_e) &= \frac{2\pi}{\hbar} \int \mathrm{d}N_f\, \delta(E_{Tf} - E_{Ti} \pm \hbar\omega(k)) |\langle k_e' | H_{ep} | k_e \rangle|^2 \\ &= \frac{e^2 \epsilon_0}{4\pi} \sum_\nu \int \mathrm{d}^2 k\, \frac{1}{\omega_\nu(k) k^2} |F_\nu(k)|^2 \delta(E_{Tf} - E_{Ti} \pm \hbar\omega_\nu(k))(N_{ph} + \tfrac{1}{2} \mp \tfrac{1}{2}) \delta_{k_e, k_e' \mp k} \end{aligned} \tag{14}$$

with

$$F_\nu(k) = \int_{-\infty}^{+\infty} \mathrm{d}z\, \Psi_f^*(z) E_k^\nu(k, z) \Psi_i(z) \tag{15}$$

where the upper (lower) sign is for phonon emission (absorption), and i (f) denotes initial (final) state. E_T is electron energy and taken to be $E + (\hbar^2 k_e^2/2m^*)$, where m^* is the

effective mass of an electron in the xy plane and E is the electron subband energy. $\Psi(z)$ is the normalized wavefunction. N_{ph} stands for the number of phonons.

For intrasubband scattering within the first subband, we consider the scattering rate W_{11} for phonon emission. Assuming that the electron energy is just enough to emit one interface phonon, we can obtain

$$W_{11}(k_{11}) = \sum_{\nu} \frac{e^2\epsilon_0}{2\omega_\nu(k_{11})k_{11}} \left(\frac{\hbar^2}{m^*}k_{11} - \hbar \frac{d\omega_\nu}{dk}\bigg|_{k=k_{11}} \right)^{-1} |F_\nu(k_{11})|^2 (N_{ph}+1) \tag{16}$$

where k_{11} satisfies

$$(\hbar^2/2m^*)k_{11}^2 - \hbar\omega_\nu(k_{11}) = 0. \tag{17}$$

For the intersubband transition between the first and second subbands, we consider the scattering rate W_{21} still for phonon emission. Assuming that the electron is initially at the bottom of the second subband, we have

$$W_{21}(k_{21}) = \sum_{\nu} \frac{e^2\epsilon_0}{2\omega_\nu(k_{21})k_{21}} \left(\frac{\hbar^2}{m^*}k_{21} - \hbar \frac{d\omega_\nu}{dk}\bigg|_{k=k_{21}} \right)^{-1} |F_\nu(k_{21})|^2 (N_{ph}+1) \tag{18}$$

where k_{21} satisfies

$$(\hbar^2/2m^*)k_{21}^2 + \hbar\omega_\nu(k_{21}) - (E_2 - E_1) = 0 \tag{19}$$

and $(E_2 - E_1)$ is the energy difference between the first and second subbands.

4. Results and discussion

In order to understand the effect of the interface component roughness on phonon vibrational modes and electron–interface phonon scattering and to make a comparison with electron relaxation experiments done by Tatham *et al* (1989) and Seilmeier *et al* (1987), we have calculated interface phonon modes and related electron–interface phonon intrasubband and intersubband scattering in an ideal quantum-well structure without roughness and in a real one with roughness, respectively. The ideal one is a $Ga_{0.64}Al_{0.36}As/GaAs/Ga_{0.64}Al_{0.36}As$ single-quantum-well structure with the well width L and infinite $Ga_{0.64}Al_{0.36}As$ barrier layers. The real one is presented by using a model quantum-well structure that has a GaAs layer with two different component interface layers on each side in the well region, i.e. a $(Ga_{0.64}Al_{0.36}As)_\infty/[(Ga_{1-x_2}Al_{x_2}As)_{p_2}$–$(Ga_{1-x_1}Al_{x_1}As)_{p_1}]/(GaAs)_{p_0}/[(Ga_{1-x_1}Al_{x_1}As)_{p_1}$–$(Ga_{1-x_2}Al_{x_2}As)_{p_2}]/(Ga_{0.64}Al_{0.36}As)_\infty$ quantum-well structure. The widths of GaAs, $Ga_{1-x_1}Al_{x_1}As$ and $Ga_{1-x_2}Al_{x_2}As$ layers are respectively p_0L, p_1L and p_2L under the condition $p_0 + 2p_1 + 2p_2 = 1$. For $Ga_{1-x}Al_xAs$ material, the potential height $V(x)$ (in units of eV) and the optical dielectric constant $\epsilon_\infty(x)$ have, respectively, the forms (Adachi 1986)

$$V(x) = (1.115x + 0.37x^2)Q \tag{20}$$

and

$$\epsilon_\infty(x) = 10.89 - 2.73x \tag{21}$$

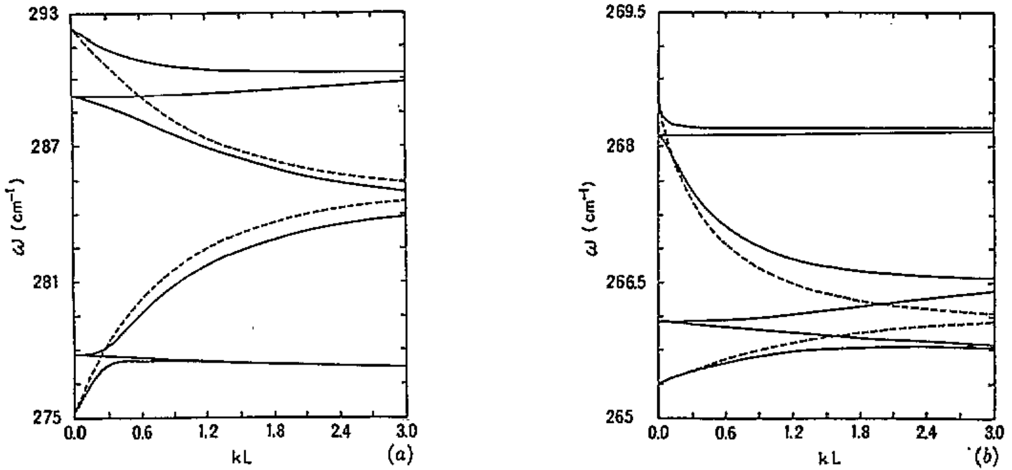

Figure 1. Dispersion relations of the interface LO modes (a) and interface TO modes (b) (see the text) in model quantum-well structures of $(Ga_{0.64}Al_{0.36}As)_\infty/[(Ga_{0.7}Al_{0.3}As)_{p_2}-(Ga_{0.94}Al_{0.06}As)_{p_1}]/(GaAs)_{p_0}/[(Ga_{0.94}Al_{0.06}As)_{p_1}-(Ga_{0.7}Al_{0.3}As)_{p_2}]/(Ga_{0.64}Al_{0.36}As)_\infty$ with $p_0 = 0.6$, $p_1 = 0.1$ and $p_2 = 0.1$ (full curves). The broken curves represent ones in the ideal structure with $p_0 = 1$ and $p_1 = p_2 = 0$.

where Q is the conduction-band offset parameter and, in general, is taken to be 0.6. The corresponding LO and TO phonon frequencies $\omega_L(x)$ and $\omega_T(x)$ (in units of cm^{-1}) of GaAs type have the forms (Adachi 1986)

$$\omega_L(x) = 292.37 - 52.83x + 14.44x^2 \tag{22}$$

and

$$\omega_T(x) = 268.50 - 5.16x - 9.36x^2 \tag{23}$$

respectively. The effective mass $m(x)$ (in units of free electron mass) of an electron is as follows:

$$m(x) = 0.067 + 0.083x. \tag{24}$$

Using formulae obtained in section 2, the dispersion relations and the electric field component $E_k(k, z)$ of the interface modes have been obtained. The dispersion curves for the model quantum-well structure mentioned above with $p_0 = 0.6$, $p_1 = p_2 = 0.1$, $x_1 = 0.06$ and $x_2 = 0.3$ have been plotted in figures 1(a) and 1(b). It can be seen that as kL approaches zero the limiting frequencies approach the LO and TO frequencies of the GaAs, $Ga_{0.94}Al_{0.06}As$, $Ga_{0.7}Al_{0.3}As$ and $Ga_{0.64}Al_{0.36}As$ material; however, as kL approaches infinity the limiting frequencies approach 290.81, 284.07, 276.54, 268.27, 266.71 and 265.68 cm^{-1}, which are not shown in the figures. There are six interface modes with frequency magnitude between $\omega_{LO}(0)$ and $\omega_{LO}(0.36)$ and six interface modes with frequency magnitude between $\omega_{TO}(0)$ and $\omega_{TO}(0.36)$. For simplicity, we denote them as interface LO modes and interface TO modes, respectively. The dispersion curves for the ideal quantum-well structure are also given for the sake of comparison. It is clearly shown that there are different dispersion relations of the interface modes for a different interface roughness. In figure 2, the electric field components E_k corresponding to six GaAs-type interface LO modes are given for the model structure. They are much more important than the interface TO modes for the electron–phonon scattering induced by Frölich interaction. Three of them are symmetric and the others antisymmetric.

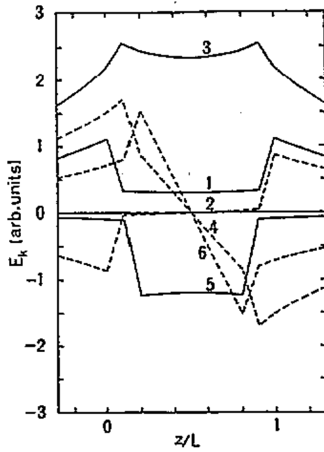

Figure 2. Electric field components E_k of interface LO modes with $kL = 1$ as a function of z in the same model structure as that in figure 1. The numbers on the curves present the frequency in order of increasing magnitude. It is the same in figures 3 and 4.

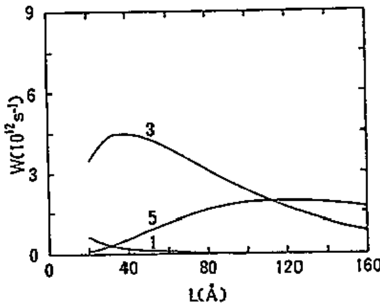

Figure 3. Intrasubband scattering rate of odd interface LO modes as a function of well width L in the same model structure as that in figure 1 (curves as in figure 2).

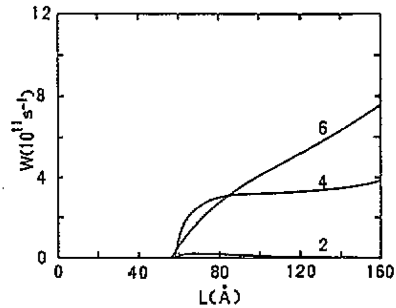

Figure 4. Intersubband scattering rate of even interface LO modes as a function of well width L in the same model structure as that in figure 1 (curves as in figure 2).

In figures 3 and 4 the intrasubband and intersubband scattering rates divided by $(N_{ph}+1)$ in the same model quantum-well structure as used above are given for each interface LO mode, which is in the order of increasing magnitude of frequency. It is found that only odd-number interface modes with symmetric $E_k(k, z)$ contribute to the intrasubband scattering and only even-number interface modes with antisymmetric $E_k(\boldsymbol{k}, z)$ contribute to the intersubband scattering. As shown in figure 2, the frequencies of modes 1 and 2 are near $\omega_{LO}(0.36)$ (bulk LO frequency of $Ga_{0.64}Al_{0.36}As$ barrier); thus the parts inside the well of these two modes are much less than that outside of the well. The wavefunction $\Psi_1(z)$ of the first subband is mostly confined in the well; therefore the contribution of these two modes to scattering rates is relatively small for any kind of scattering. The potential barrier height for an electron of the $Ga_{0.64}Al_{0.36}As$ layer is about 270 meV. There is only one subband energy level and no intersubband scattering for such a barrier height with the well width L less than about 55 Å.

In figure 5, intrasubband scattering rates divided by $(N_{ph} + 1)$ are given for interface modes in model quantum-well structures with $x_1 = 0.06$, $x_2 = 0.3$ and (i) $p_0 = 1$, $p_1 = p_2 = 0$, (ii) $p_0 = 0.8$, $p_1 = p_2 = 0.05$ and (iii) $p_0 = 0.6$, $p_1 = p_2 = 0.1$. In order to show the difference between finite and infinite barrier heights, the scattering rates are also given in the figure for the case (iv) $p_0 = 1$, $p_1 = p_2 = 0$ with an infinite barrier height. It

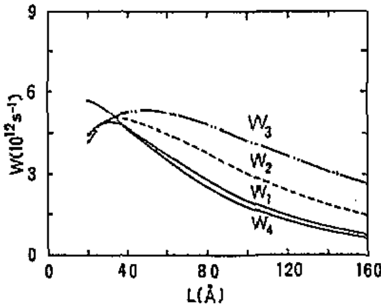

Figure 5. Intrasubband scattering rates as a function of well width L for (i) $p_0 = 1$, $p_1 = p_2 = 0$ (full curve W_1), (ii) $p_0 = 0.8$, $p_1 = p_2 = 0.05$ (broken curve W_2) and (iii) $p_0 = 0.6$, $p_1 = p_2 = 0.1$ (chain curve W_3) with a finite barrier height, and (iv) $p_0 = 1$, $p_1 = p_2 = 0$ (full curve W_4) with an infinite barrier height (see the text).

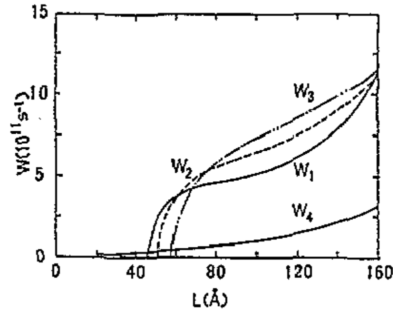

Figure 6. Intersubband scattering rates as a function of well width L for (i) $p_0 = 1$, $p_1 = p_2 = 0$ (full curve W_1), (ii) $p_0 = 0.8$, $p_1 = p_2 = 0.05$ (broken curve W_2) and (iii) $p_0 = 0.6$, $p_1 = p_2 = 0.1$ (chain curve W_3) wth a finite barrier height, and (iv) $p_0 = 1$, $p_1 = p_2 = 0$ (full curve W_4) with an infinite barrier height (see the text).

is readily seen that intrasubband scattering rates in the model quantum-well structures (ii) and (iii) are much larger than those in the ideal quantum-well structure (i). The wider the interface layers, the larger are the intrasubband scattering rates. Since different interface roughness corresponds to different dispersion relation, the k_{11} determined by equation (17) and corresponding electric field component E_k and overlap integral $F_\nu(k_{11})$ in quantum-well structures with interface roughness will be quite different from those in the ideal quantum-well structure. Though the difference in the first electron subband wavefunction between quantum-well structures with and without interface roughness is small, the difference in scattering rates can be large. Previous studies (Ridley 1989, Rudin and Reinecke 1990) have shown that interface phonon scattering is a more important scattering mechanism in narrow quantum-well structures compared with confined LO phonon scattering. Therefore, it is necessary to include the effect of interface roughness on the interface phonon modes in the discussion of electron transport in superlattice and quantum-well structures. We believe that this is one reason why the calculated electron mobility of Dharssi and Butcher (1990) in $Ga_{0.7}Al_{0.3}As/GaAs$ superlattice is too large compared with the experiments (Sibille *et al* 1987). From figure 5, it is also shown that the scattering rates for case (iv) are almost the same as those for case (i) when well width L is larger than 40 Å. Based on equations (16) and (17) we can see that k_{11} has no relation to electron subband energy level and barrier height. If the well width L is larger than 40 Å, the first electron subband wavefunction is mostly confined in the well. The difference in wavefunction $\Psi(z)$ and corresponding $F_\nu(k_{11})$ between finite and infinite barrier height approximations is small, which results in the small difference of the calculated intrasubband scattering rates in the two cases.

In figure 6, the intersubband scattering rates divided by $(N_{\rm ph} + 1)$ are given for the same model quantum-well structures as those in figure 5. We can see that the intersubband scattering rates for case (iv) are quite different from those for case (i). It shows that the infinite barrier height approximation is not the proper one to use for intersubband scattering. We can explain the results in two aspects. On the one hand, the infinite barrier height approximation gives rise to the larger energy difference $(E_2 - E_1)$ between electron subband energy levels. Since $\hbar\omega_\nu$ and $(E_2 - E_1)$ are of the same order, k_{21} and the corresponding electric field component E_k are quite different for the two cases of finite and infinite barrier height. On the other hand, electron wavefunctions of a finite barrier

height, especially that of the second subband, are more extended, quite different from the completely confined electron wavefunctions in the infinite barrier height approximation. The electric field component E_k is extended. Therefore, the infinite barrier height approximation introduces large errors in the calculation of the overlap integrals $F_\nu(k_{21})$, and thus large errors in the calculation of scattering rates. From figure 6, we can see that the intersubband scattering rates of narrow quantum-well structures (well width about 50 Å) depend strongly on the interface roughness. For narrow quantum-well structures, a small change of interface can cause a large change of electron subband wavefunction. We also find that for a wide quantum well the scattering rates in model quantum-well structures with and without interface roughness are similar and the differences between them are relatively small. It shows that the effects of interface roughness on the dispersion relation, electron subband energy levels and wavefunction can cancel each other and the intersubband scattering rate is not very sensitive to interface roughness in wide quantum-well structures. Recently, several experimental results giving information about intersubband relaxation rates in quantum-well structures have been reported (Tatham *et al* 1989, Obreli *et al* 1987, Seilmeier *et al* 1987). Time-resolved Raman anti-Stokes scattering experiments of Tatham *et al* (1989) have given an estimate for the upper bound on the intersubband relaxation time of 1 ps for a $Ga_{0.64}Al_{0.36}As/GaAs$ quantum-well structure of well width 146 Å at 30 K. Combining our calculation with the value of Rudin and Reinecke (1990) by the Huang–Zhu microscopic model (Huang and Zhu 1988a, b) for the contribution of confined LO phonon to the intersubband scattering rate, we have obtained a relaxation time of about 0.8 ps, which is in good agreement with the above experiment. It should be pointed out that an infinite barrier height approximation is used in the calculation of Rudin and Reinnecke (1990). Because confined LO phonon modes are dispersionless, the approximation leads to a relatively small error for the contribution of the confined LO phonon to the scattering rate in a wide quantum well. Seilmeier *et al* (1987) have studied the bleaching of the intersubband absorption induced by a high-intensity picosecond pump. Measured intersubband relaxation times for a $Ga_{0.65}Al_{0.35}As/GaAs$ quantum-well structure with well width of about 50 Å are of the order of 10 ps at 300 K for a subband splitting of about 150 meV, with increasing tendency of smaller well width. In such a narrow quantum well, the wavefunction of the second subband is much extended, and the contribution of the confined LO phonon to the scattering rate is very small and can almost be ignored compared with that of interface modes, which are extended. So interface phonon scattering is the dominant scattering mechanism in narrow quantum-well structures. From figure 6, we have obtained the intersubband relaxation time of about 4.3 ps for a 50 Å ideal quantum-well structure with $p_0 = 1$ and $p_1 = p_2 = 0$. But for a 50 Å model quantum-well structure with interface roughness, the scattering rates can be smaller, which corresponds to a longer relaxation time. Then, one would expect that the calculated results can be in good agreement with the experiment (Seilmeier *et al* 1987) as the proper interface roughness is considered. In addition, we have studied the dependence of scattering rates on the conduction-band offset parameters Q for a narrow quantum-well structure in which the second energy level E_2 is very close to the barrier height. The intersubband scattering rates and relaxation times in a 50 Å ideal quantum-well structure with $p_0 = 1$ and $p_1 = p_2 = 0$ have been calculated for different Q. It is found that the difference between the second energy level E_2 and the barrier height in the structure is equal to 1.12, 0.38 and 0.15 meV for $Q = 0.55$, 0.53 and 0.52, respectively, and that the smaller the difference, the more extended is the envelope wavefunction of the second subband. Then, it is obtained that the relaxation time is respectively 6.9, 10.8 and 16.2 ps for $Q = 0.55$, 0.53 and 0.52. It shows that the relaxation time in narrow quantum-well structures is sensitive to the conduction-band offset parameter Q. Therefore,

the measurement of the intersubband relaxation time may offer a method to check the value of Q.

It should be important and interesting to study the variation of intrasubband and intersubband scattering rates with x_1 and x_2 in the model structure. For the structure with $p_0 = 0.6$ and $p_1 = p_2 = 0.1$, we have also calculated the scattering rates for different well width L with $x_1 = 0.12$, $x_2 = 0.24$ and $x_1 = 0.18$, $x_2 = 0.18$, respectively. It is found that the variation of intrasubband scattering rate with L is almost the same as W_3 shown in figure 5, and that there is almost no difference between the intersubband scattering rates and W_3 shown in figure 6 in the region $L < 120$ Å and there is a slight difference in the region $L > 120$ Å. The difference is about 15% at $L = 160$ Å. Therefore, we have chosen only one set $x_1 = 0.06$ and $x_2 = 0.3$ in the figures under discussion.

5. Conclusion

In conclusion, we have for the first time taken into account the effect of interface roughness on electron–interface phonon scattering rates. It has been shown that interface roughness can lead to a steep increase in the intrasubband scattering rate, so it should be considered in a good description of electron transport in quantum-well structures, and that the intersubband scattering rates and relaxation times in a narrow quantum well are very sensitive to interface roughness. The validity of the infinite barrier height approximation is also tested. Calculated results have shown that it is a fairly good approximation for intrasubband scattering, and it can introduce a larger error, in particular, in narrow quantum-well structures for intersubband scattering. A calculation with finite barrier height is needed for intersubband scattering. Based on what we have mentioned above, the experiments (Tatham *et al* 1989, Seilmeier *et al* 1987, Sibille *et al* 1987) can be explained better. Finally, it is interesting to point out that our calculation formula is convenient and powerful not only for the structures mentioned above but also for other kinds of structures in the calculation of electron–phonon scattering and optic phonon Raman scattering, and that further experimental data are needed to check the model used here.

References

Adachi S 1986 *J. Appl. Phys.* **58** R1
Chen R, Lin D L and George T F 1990 *Phys. Rev.* B **41** 1435
Dharssi I and Butcher P N 1990 *J. Phys.: Condens. Matter* **2** 119
Fuchs R and Kliewer K L 1965 *Phys. Rev.* A **140** 2076
Huang K and Zhu B 1988a *Phys. Rev.* B **38** 2183
—— 1988b *Phys. Rev.* B **38** 13377
Jusseraud B, Paquet D and Regreny A 1984 *Phys. Rev.* B **30** 6245
Licari J J and Evrard R 1977 *Phys. Rev.* B **15** 2254
Obreli D Y, Wake D R, Klein M V, Kelm J, Henderson T and Morkoc H 1987 *Phys. Rev. Lett.* **59** 696
Ridley B K 1989 *Phys. Rev.* B **39** 5282
Rudin S and Reinecke T L 1990 *Phys. Rev.* B **41** 7713
Seilmeier A, Huber H J, Abstreiter G, Weimann G and Schlapp W 1987 *Phys. Rev. Lett.* **59** 1345
Sibille A, Palmier J, Minot C, Harmand J and Dubon-Chevallier C 1987 *Superlatt. Microstruct.* **3** 553
Sood A K, Menéndez J, Cardona M and Ploog K 1985 *Phys. Rev. Lett.* **54** 2115
Stroscio M A, Lafrate G J, Kim K W, Littlejohn M A, Goronkin H and Maracas G N 1991 *Appl. Phys. Lett.* **59** 1093
Tatham M C, Ryan J F and Foxon C T 1989 *Phys. Rev. Lett.* **63** 1637
Wendler L 1985 *Phys. Status Solidi* b **129** 513
Zhu J L, Tang D H and Xiong J J 1989 *Phys. Rev.* B **39** 8609